ORIGINAL ARTICLE

Energy-Saving and Punctuality Combined Velocity Planning for the Autonomous-Rail Rapid Tram with Enhanced Pseudospectral Method

Jinxiang Wang[1], Dongming Han[1], Yongjun Yan[1], Neng Liu[1], Ning Sun[2] and Guodong Yin[1*]

Abstract

Autonomous-rail rapid transit (ART) is a new medium-capacity rapid transportation system with punctuality, comfort and convenience, but low-cost construction. Combined velocity planning is a critical approach to meet the requirements of energy-saving and punctuality. An ART velocity pre-planning and re-planning strategy based on the combination of punctuality dynamic programming (PDP) and pseudospectral (PS) method is proposed in this paper. Firstly, the longitudinal dynamics model of ART is established by a multi-particle model. Secondly, the PDP algorithm with global optimal characteristics is adopted as the pre-planning strategy. A model for determining the number of collocation points of the real-time PS method is proposed to improve the energy-saving effect while ensuring computation efficiency. Then the enhanced PS method is utilized to design the velocity re-planning strategy. Finally, simulations are conducted in the typical scenario with sloping roads, traffic lights, and intrusion of the pedestrian. The simulation results indicate that the ART with the proposed velocity trajectory optimization strategy can meet the punctuality requirement, and obtain better economy efficiency compared with the punctuality green light optimal speed advisory (PGLOSA).

Keywords Autonomous-rail rapid tram (ART), Velocity trajectory planning, Dynamic programming, Pseudospectral method

1 Introduction

Urban commuters are confronted with the growing problem of traffic congestion [1]. Urban rail transit systems are very important for public transportation in large and medium-sized cities because of their advantages in transportation capacity, efficiency, punctuality, safety, and environmental friendliness [2, 3]. Due to the different

factors such as population, economy, terrain, and traffic conditions in different cities, demands on the rail transit systems are also diverse. Thus, some innovative transportation products with new technologies and modes have emerged, such as autonomous-rail rapid transit (ART) [4, 5].

Powered by electric motors, ART combines the features of urban rail transit and urban surface public transportation, which requires ART to meet the requirements of economy and punctuality simultaneously. After solving the problem of guaranteeing accurate tracking of a fixed line [6], various driving strategies can be adopted for ART to travel from the departure to the destination. In the operation of urban rail transit systems, the traction energy consumption of trains accounts for more than half

*Correspondence:
Guodong Yin
ygd@seu.edu.cn
[1] School of Mechanical Engineering, Southeast University, Nanjing 211189, China
[2] School of Automotive and Traffic Engineering, Nanjing Forestry University, Nanjing 210037, China

Wang *et al. Chinese Journal of Mechanical Engineering*   (2023) 36:82

Page 2 of 13

of the total energy consumption. And the rest of energy consumption is mostly caused by infrastructure, such as ventilation systems, lighting systems, drainage systems, elevator equipment, etc. [7]. Therefore, the energy-efficient driving method can achieve a better energy-saving effect without changing the stations, lines, and operation diagram, which is an effective way to reduce the overall energy consumption and operation cost of the existing urban rail transit [8].

On the other hand, different from traditional rail transit, ART is used for surface public transportation, which is not subject to the physical constraints of the traditional rails and has a relatively open driving environment including traffic lights. Besides, the public traffic participant, such as pedestrians and general vehicles, may intrude into the virtual rail. To satisfy the demands of energy-saving and punctuality in such a situation, a real-time optimization algorithm is needed for velocity planning. To sum up, the velocity profile of the ART between adjacent stations should be planned to ensure the performances in terms of economy and punctuality, by considering the constraints of vehicle dynamics, road conditions, traffic lights, and collision avoidance with other traffic participants.

The task of velocity planning is to calculate a reasonable and safe speed distribution on the future path, according to the states of the ART, the expected path, and environmental information. Some researches have been conducted on velocity planning to achieve the economy and punctuality of vehicles and trains. Pontryagin's maximum principle (PMP) was used to solve the problem of optimal train speed profile planning for different driving conditions in Refs. [9, 10]. A real-time strategy for speed planning based on PMP and Lagrange multiplier technique was proposed in Ref. [11] to improve the performance of punctuality and energy efficiency of the high-speed train. However, the complex road environments for ART such as traffic lights, and other traffic participants must be considered in velocity planning, and the difficulty of solving the problem based on PMP will be greatly increased. Dynamic programming (DP) is a globally optimal algorithm that is usually utilized to design energy-efficient driving strategies. The energy consumption and the arrival time of the train were taken as the optimization objectives to develop control strategies for the energy-saving operation in Refs. [12, 13]. Haahr et al. [14] proposed a DP algorithm to optimize the economy of trains, taking into account the road altitude variation, the velocity, and the time constraints. Hellström et al. [15] developed a DP-based forward-looking control strategy for heavy-duty diesel trucks by comprehensively considering the energy consumption and travel time. The energy-driving strategy based on DP is proposed in Refs. [16, 17],

considering the road slope for fuel vehicles and electric vehicles, respectively. Asadi et al. [18] predicted the optimal speed trajectory to improve the driving economy of vehicles, considering the phase and time information of traffic lights. As a result, the vehicles passed within the green time, and the extra travel time and fuel consumption are reduced. Although the global optimum can be obtained by DP, the solving efficiency will be greatly reduced in the phenomenon of "dimension disaster" when the problem becomes complex and the optimization variables increase.

Nonlinear model predictive control (NMPC) was also applied to generate fuel-saving speed trajectories considering a short speed preview of the preceding vehicle [19]. However, NMPC is dissatisfactory in optimizing economy and comfort with its limitation of prediction horizon [20–22]. On the other hand, the pseudospectral (PS) method was also adopted in Ref. [23] to plan the optimal trajectory with consideration of the indicators such as running comfort, punctuality, and economy. Xiao et al. [24] proposed a speed optimization model combining energy management with operation control strategies for high-speed train systems and used the PS method for achieving energy-saving and efficient operation. Xu et al. [25] proposed a method to compute the optimal speed profiles for an eco-driving system based on PS, which has the advantages of high accuracy and fast convergence. In addition, in Refs. [26, 27], the economic driving strategy for vehicles at signalized intersections with traffic lights was designed based on the PS method, which improved the energy efficiency of vehicles. In these studies, the optimality of the solution is closely related to the distribution of collocation points of the PS method. Hence, the same distribution of collocation points does not always appropriate for multiple traffic scenarios. In conclusion, none of the above methods can simultaneously satisfy the real-time and optimality of velocity trajectory planning. Therefore, there is an urgent need to study the real-time optimization algorithm of velocity planning to ensure that the driving objectives of ART such as safety, punctuality, and economy can be achieved under complex driving conditions.

In this paper, a real-time optimization strategy for ART velocity trajectory planning is proposed to achieve a punctual and energy-saving cruise between two stations. The main contributions of this paper are as follows. Firstly, the global pre-planning velocity trajectory is derived with PDP considering the dynamics model of ART, real road information, punctuality constraints, and traffic lights. Secondly, a model for determining the number of collocation points is established to balance the energy-saving effect and computation efficiency for the proposed PS-based velocity planning method. Thirdly,

the enhanced PS-based real-time method is applied to re-plan the velocity trajectory of the remaining route when the operation of ART is intruded on by other traffic participants.

In this paper, the main contents of the longitudinal velocity planning of ART are as follows. In Section 2, the longitudinal dynamics model of ART is established. In Section 3, the PDP and PS-based strategy of velocity trajectory planning for ART is proposed. In addition, the model to determine the number of collocation points for the PS method is established. In Section 4, the PreScan/Trucksim/Simulink co-simulation environment is designed, and the simulation results are analyzed to demonstrate the effectiveness of the proposed strategy. Section 5 is the conclusion of this paper.

2 Framework of Energy-Saving and Punctuality Optimization Velocity Planning for ART

2.1 Framework of the Velocity Planning Strategy

The framework of the velocity planning strategy for ART is shown in Figure 1, including traffic information, the ART dynamics model, the velocity pre-planning module, and the velocity re-planning module. The traffic information from the real road maps provides emergencies, road slope, and signal phase and timing (SPaT) for ART, which are considered constraints in velocity planning. The objective function of the optimization problem reflecting

the energy consumption is determined by the dynamics model of ART. The PDP and PS methods are adopted for velocity pre-planning and re-planning, respectively.

Under normal situations, ART follows the velocity trajectory pre-planned by PDP to improve punctuality and economic performance. Nevertheless, ART switches to follow the velocity trajectory re-planned by the PS method when the route of ART is intruded on by pedestrians, low-speed vehicles, or other traffic participants. Considering the signalized intersection, the whole journey is divided into several segments, and the velocity trajectory is planned sequentially.

2.2 Longitudinal Dynamics Model of ART

The single-particle model [28–30] and the multi-particle train model [31, 32] can be used to model the dynamics for train operation control. With the multi-particle model, the forces of each carriage can be analyzed separately, and the slope change of the road can be considered [33, 34], thus the control accuracy can be improved.

In this paper, the multi-particle dynamics model is selected to compensate for the shortage of single-particle models in simple modeling and incomplete analysis. ART is considered a "particle chain", and each carriage is treated as a particle. Then, the forces of each carriage can be analyzed separately, which makes the dynamics model more accurate. On the other hand, the gradient
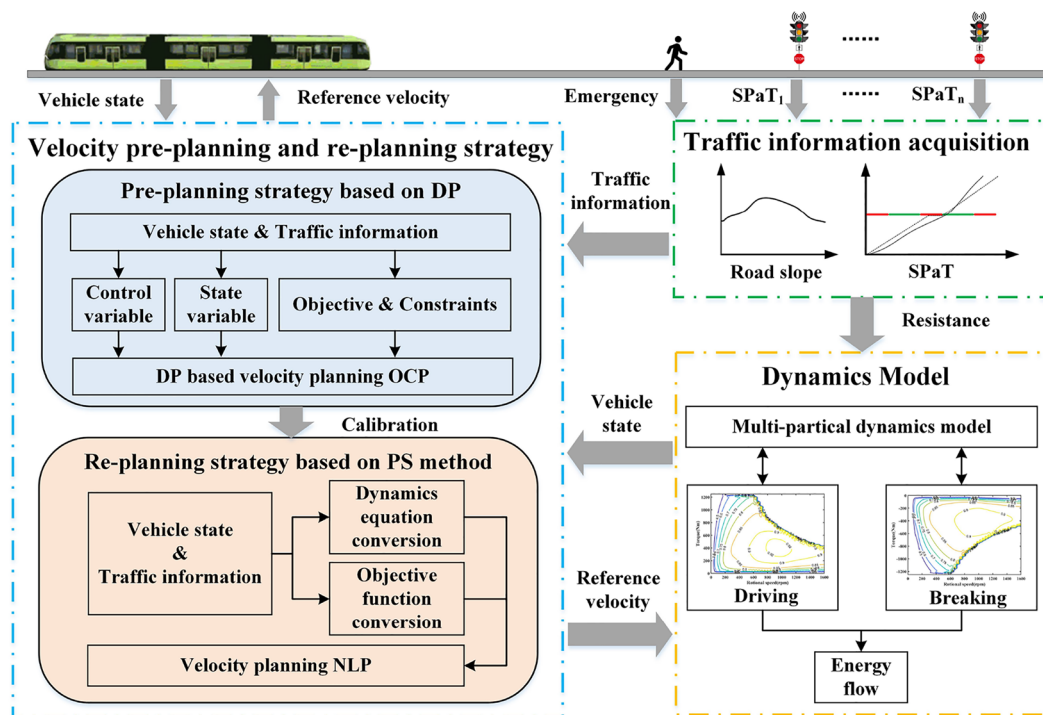
Figure 1 The framework of the velocity planning strategy for ART considering punctuality and economy

Wang *et al. Chinese Journal of Mechanical Engineering*   (2023) 36:82

Page 4 of 13

resistance based on the multi-particle dynamics model changes gradually at different slope sections, therefore the planned velocity of the ART can be smoothed.

To establish a practical and computable dynamics model for the ART, it is necessary to make the following assumptions: The forces generated by the articulation are not considered, and the mass of each carriage is identical. To ensure the continuity of velocity, the longitudinal acceleration of each carriage is regarded as identical. In addition, the lateral motion and the vertical vibration of ART are ignored during the longitudinal velocity planning.

Based on the assumptions, the multi-particle dynamics model of the ART is demonstrated as the schematic diagram in Figure 2, where F_t is the driving force produced by the six identical motors. The resistance is composed of air resistance F_w, rolling resistance $F_{f,i}$ and gradient resistance $F_{g,i}$. G_i and θ_i denote the gravity and slope angle of carriage i ($i = 1, 2, 3$), respectively. The interaction force of adjacent carriages is equal, where $F_{1,2} = F_{2,1}$ and $F_{2,3} = F_{3,2}$. According to the force analysis, the longitudinal dynamics model of ART for velocity planning is shown as [35]:

$$
\begin{aligned}
M\frac{\mathrm{d}v}{\mathrm{d}t} &= F_t - F_w - \sum_{i=1}^{3} F_{f,i} - \sum_{i=1}^{3} F_{g,i} \\
&= \frac{6T_m}{R_t} - \frac{1}{2}\rho C_d A_F v^2 \\
&\quad - \frac{M}{3} g f_r (\cos\theta_1 + \cos\theta_2 + \cos\theta_3) \\
&\quad - \frac{M}{3} g (\sin\theta_1 + \sin\theta_2 + \sin\theta_3),
\end{aligned}
\tag{1}
$$

where C_d denotes the air resistance coefficient; A_F denotes the front area of the first carriage; v denotes the longitudinal velocity of ART; f_r is the rolling resistance coefficient; M denotes the total mass of ART; g denotes gravitational acceleration; T_m denotes the torque of one motor; R_t denotes the radius of tire.

The change in battery power reflects the energy consumption of each motor. The power model of each motor in driving and breaking condition is calculated by
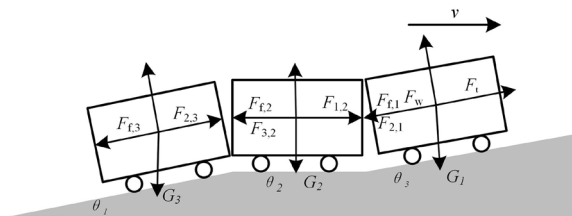
Figure 2 Force analysis of the ART

$$
P_m = \begin{cases} T_m \omega_m / \eta_m & T_m > 0, \\ T_m \omega_m \eta_e & T_m < 0, \end{cases}
\tag{2}
$$

where P_m denotes the power of motor; ω_m denotes the rotational speed. η_m and η_e denote the output efficiency and generation efficiency of the motor, respectively. In some researches about the ecological driving of electric vehicles, the battery model is simplified by setting the electrochemical conversion efficiency as a constant or ignoring electrochemical reaction [36, 37]. Therefore, the battery power equals P_m, and the energy consumption can be obtained as

$$
\Delta Q = \int P_m \, \mathrm{d}t,
\tag{3}
$$

where ΔQ represents the electricity consumption.

3 Velocity Trajectory Optimization Strategy Combined with Pre-planning and Re-planning Method

3.1 Pre-planning of the Global Optimal Velocity

DP is an optimization algorithm based on the Bellman optimization principle, which is an effective mathematical method to solve the optimal control problem (OCP). With DP, the complex multivariable optimization problems are solved in two steps. First, the optimal solution of each stage is obtained, and second, the algorithm of the recursive call is used to obtain the optimal solution for complex problems. DP divides the optimal solution into discrete stages and transforms the whole optimization problem into N subproblems. Then, the state variables and the control decisions of each subproblem are described.

The longitudinal speed planning problem in this paper is an N-level decision-making process, in which the whole operation process of ART can be divided into N stages. Then the optimal control torque of each stage can be solved, so that the speed can be transferred continuously between each stage. For each sub-stage, the electricity consumption and driving time of the initial state in the transfer process should be calculated accordingly. In summary, the optimal control variables are calculated by reverse solving, and then the optimal control set u_k ($k = 0, 1, ..., N-1$) and the state set v_k are found by forward optimization.

The electricity consumption and travel time of the train between adjacent stations are selected as objective functions when constructing the optimal control problem of ART. In order to eliminate the magnitude difference between time and energy index, a weight coefficient α is set for the travel time. Therefore, the OCP of the system can be obtained as Eq. (4), where T_{min} and T_{max} represent the torque limits of the motor; v_{min} and v_{max} represent

Wang *et al. Chinese Journal of Mechanical Engineering*　　(2023) 36:82

Page 5 of 13

the limits of the cruising velocity; the state transition function f is derived from Eq. (1). t_k is the travel time of stage k. $j_{\max}$ denotes the limitation of jerk. v_{nmax} and v_{nmax} denote the minimum and maximum velocity when ART arrives at the next station. t_{arrival} denotes the arrival time. α denotes the weight coefficient of time in the objective function.

When the value of α is small, the weight of travel time in the objective function is small, resulting in longer travel time accordingly, and vice versa. The dichotomy method can be adopted to adjust the weight coefficient of time optimization to meet the requirement of punctuality, and thus realizes the punctuality dynamic programming (PDP). The procedures of the proposed PDP based on dichotomy method are summarized in Figure 3.

$$
\begin{cases}
\min_{T_{\mathrm{m}}(k)} (J), \\
J = \sum_{k=0}^{N-1} \Delta Q(k) + \alpha \sum_{k=0}^{N-1} t_k, \\
\text{s.t. } v(k+1) = f(v(k), T_{\mathrm{m}}(k)), \\
T_{\min} \le T_{\mathrm{m}}(k) \le T_{\max}, \\
v_{\min} \le v(k) \le v_{\max}, \\
\left| j(k) \right| \le j_{\max}, \\
v_{\mathrm{nmin}} \le v(N) \le v_{\mathrm{nmax}}, \\
t_{\mathrm{arrival}} = \sum_{k=0}^{N-1} t_k = \sum_{k=0}^{N-1} \dfrac{2\Delta s}{v(k+1)+v(k)}.
\end{cases}
\tag{4}
$$

3.2 Re-planning of Velocity Based on PS Method

During the operation of ART, unexpected emergencies such as pedestrian intrusion and traffic jams are inevitable. Therefore, a real-time velocity planning method is needed to re-plan the longitudinal velocity trajectory. PDP is a global optimization algorithm, but it cannot be

Figure 3 Procedures of PDP algorithm

adopted as a real-time strategy for re-planning because of the low computational efficiency and poor real-time performance.

Remark 1: If the ART cruise is not disturbed by emergencies, ART will follow the pre-planning velocity all the time to achieve the most energy-saving cruise.

The OCP for velocity re-planning can be solved with the PS method, which belongs to a special kind of direct method. The PS method has the advantages of fast convergence, large radius of convergence, high precision of solution, and low sensitivity of initial value. Its numerical solution has been proved theoretically to satisfy optimality [38]. Based on the PS method, the optimal control model of the longitudinal velocity planning problem is reconstructed and transformed into nonlinear programming (NLP), which can be solved efficiently.

The objective function is designed by the energy consumption function. In addition, the constraints of OCP are set to meet the requirements of ART in safety and punctuality. The constrains include velocity range $v_{\min} \le v_k \le v_{\max}$, torque range $T_{\min} \le T_k \le T_{\max}$, and the target cruising time $t_{\mathrm{f}} = t_{\mathrm{target}}$. To sum up, the OCP for velocity re-planning of ART is defined as follows:

$$
\min J = \int_0^{t_{\mathrm{f}}} P(v, T_{\mathrm{m}})\mathrm{d}t,
$$

$$
\text{s.t. } \dot{x} = \begin{pmatrix} \dot{s} \\ \dot{v} \end{pmatrix} = \begin{pmatrix} 0 & 1 \\ 0 & \dfrac{-F_{\mathrm{R}}}{M} \end{pmatrix} \begin{pmatrix} s \\ v \end{pmatrix} + \begin{pmatrix} 0 \\ \dfrac{1}{R_{\mathrm{t}}M} \end{pmatrix} T_{\mathrm{m}},
$$

$$
\begin{cases}
v(t_0) = v_0, \\
s(t_0) = S_0, \\
s(t_{\mathrm{f}}) = S_{\mathrm{f}}, \\
v_{\mathrm{nmin}} \le v(t_{\mathrm{f}}) \le v_{\mathrm{nmax}},
\end{cases}
$$

$$
\begin{cases}
S_0 \le s(t) \le S_{\mathrm{f}}, \\
v_{\min} \le v(t) \le v_{\max}, \\
T_{\min} \le T_m(t) \le T_{\max},
\end{cases}
\tag{5}
$$

where distance $s(t)$ and velocity $v(t)$ are state variables; t_0 denotes the starting time; t_{f} denotes the terminal time of OCP. The torque of the motor $T_{\mathrm{m}}(t)$ is taken as control variable. S_0 represents the beginning position, and S_{f} represents the terminal position. v_0 represents the initial velocity of ART.

Different types of PS methods have different advantages. The OCP of ART contains non-free boundary conditions, such as the initial velocity, initial position, arrival time, and limits of the cruising velocity of ART. The Legendre PS method is adopted in this paper because of its better performance for solving the problem of ART with non-free boundary conditions, while
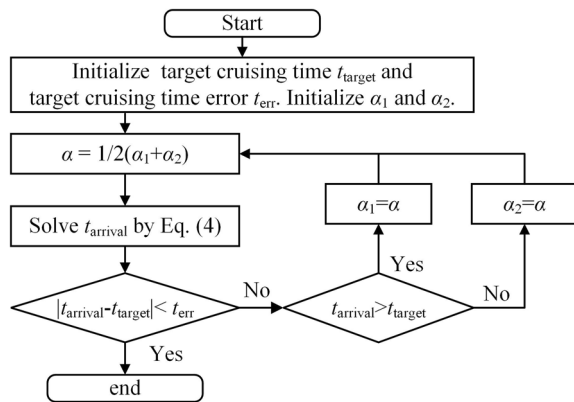
the Gauss PS method and Radau PS method may not converge in these conditions [25].

The state and control variables are scattered on Legendre Gauss Lobatto (LGL) collocation points, and approximated by Lagrange interpolating polynomials. The differential dynamic equation constraints are transformed into algebraic constraints on the interpolating points. The integral part in the objective function is calculated by the LGL integral. The detailed transformation process is described as follows.

3.2.1 Approximation of State and Control Variables

τ_k ($k = 0, 1, \ldots N$) denotes the LGL collocation point. It is the root of polynomial $(1 - \tau^2)\dot{P}_N(\tau)$ as well. P_N is the Legendre polynomial of order N, which is described as

$$P_N(x) = \frac{1}{2^N N!} \frac{d^N(x^2 - 1)^N}{dx^N}. \tag{6}$$

The collocation points $\tau_k \in [-1, 1]$. Therefore, the time domain t_k needs to be transformed into

$$\tau_k = \frac{2t_k - (t_f + t_0)}{t_f - t_0}, \tag{7}$$

where t_f equals to the target cruising time t_{target}. Then the state variable $x(\tau_k)$ and control variable $u(\tau_k)$ are approximated as:

$$x(\tau_k) \approx X(\tau_k) = \sum_{i=0}^{N} L_i(\tau_k)X_i, \tag{8}$$

$$u(\tau_k) \approx U(\tau_k) = \sum_{i=0}^{N} L_i(\tau_k)U_i, \tag{9}$$

where X_i and U_i are the interpolating points of state variables and control variables, respectively. L_i ($i = 0, 1, \ldots, N$) denotes the Lagrange interpolating polynomial of order N, with the expression:

$$L_i(\tau) = \prod_{j=0, j \neq i}^{N} \frac{\tau - \tau_i}{\tau_i - \tau_j}. \tag{10}$$

3.2.2 Transformation of Differential Dynamic Equations

By differentiating the state variables in Eq. (8), the dynamic equations can be transformed into

$$\dot{x}(\tau_k) = \sum_{i=0}^{N} \dot{L}_i(\tau_k)X_i = \sum_{i=0}^{N} D_i(\tau_k)X_i. \tag{11}$$

Specifically, the dynamic equations are expressed as:

$$\sum_{i=0}^{N} D_i(\tau_k)S_i - \frac{t_f - t_0}{2}V_k = 0, \tag{12}$$

$$\sum_{i=0}^{N} D_i(\tau_k)V_i - \frac{t_f - t_0}{2}\left(\frac{T_k}{R_t} - F_R\right) \Big/ M = 0, \tag{13}$$

where S, V, and T are the interpolating points of position, velocity and torque. $D_i(\tau_k)$ is the differential matrix [39].

3.2.3 Transformation of Objective Function

The integral part of objective function in the OCP can be approximated by the LGL integral, which is defined as

$$J \approx \frac{t_f - t_0}{2} \sum_{k=0}^{N} \omega_k P(X_k, U_k, \tau_k), \tag{14}$$

where ω_k is the integral coefficient. It is expressed as

$$\omega_k = \frac{2}{N(N + 1)[P_N^2(\tau_k)]^2}. \tag{15}$$

After transformation, the mathematical model of the NLP is obtained as:

$$\begin{aligned}
\min J &= \frac{t_f - t_0}{2} \sum_{k=0}^{N} \omega_k P(X_k, U_k, \tau_k), \\
\text{s.t.} &\sum_{i=0}^{N} D_i(\tau_k)S_i - \frac{t_f - t_0}{2}V_k = 0, \\
&\sum_{i=0}^{N} D_i(\tau_k)V_i - \frac{t_f - t_0}{2}(\frac{T_k}{R_t} - F_R)/M = 0, \\
&\begin{cases} V(\tau_0) = V_0, \\ S(\tau_0) = S_0, \\ S(\tau_N) = S_f, \\ V_{\text{nmin}} \leq V_N \leq V_{\text{nmax}}, \end{cases} \\
&\begin{cases} S_0 \leq S_k \leq S_f, \\ V_{\min} \leq V_k \leq V_{\max}, \\ T_{\min} \leq T_k \leq T_{\max}, \end{cases} \\
&k, i = 0, 1, \ldots, N,
\end{aligned} \tag{16}$$

where S, V, and T are regarded as the variables to be optimized. For the $N+1$ collocation points obtained by the PS method, $2 \times (N+1)$ interpolation points for the state variables and $(N+1)$ interpolation points for the control variables can be obtained discretely. Therefore, there are $3 \times (N+1)$ parameters to be optimized in this NLP.

3.3 Model to Determine the Number of Collocation Points

The number of collocation points of the PS method will affect the approximation accuracy of the discrete

model to the original model and thus affect the economy of re-planning velocity. However, with the number of collocation points increasing, the computation efficiency will decline. Energy optimality and computation efficiency cannot be guaranteed at the same time. To find the optimal number, the pre-planning results of PDP are taken as an optimal reference to select the optimal number of collocation points for the re-planning method based on PS. Firstly, the PDP approach is adopted to plan the velocity based on the road intercepted from the real road map. Secondly, the PS methods with different numbers of collocation points are taken to re-plan the velocity under the same conditions, and the results are compared with those based on the PDP method.

To determine the appropriate number of collocation points, both the computation time of algorithms and the planning results are considered in the model. For the planning results, the root-mean-square error (RMSE) is used to describe the differences between the velocity trajectories based on the PS method and those based on PDP. By comparing the sums of the normalized value of the computation time and the RMSE for the different numbers of collocation points, the optimal number of collocation points can be found.

The RMSE is calculated by

$$E = \sqrt{\frac{1}{N} \sum_{k=1}^{N} (v_{\text{PS},k} - v_{\text{PDP},k})^2}, \quad (17)$$

where N is the number of sampling points, which equals to the number of discrete points based on PDP; $v_{\text{PS},k}$ and $v_{\text{PDP},k}$ are values sampled from the velocity curves planned by the PS and PDP methods, respectively.

For each collocation number k_i in set $K = \{k_1, k_2, ..., k_n\}$, the computation time of PS method and RMSE are normalized by

$$\Gamma_i = \frac{t_i - t_{\min}}{t_{\max} - t_{\min}}, \quad (18)$$

$$\Psi_i = \frac{E_i - E_{\min}}{E_{\max} - E_{\min}}, \quad (19)$$

where t_i is the computation time of algorithm with k_i collocation points, and $k_i \in \{20, 30, 40, ..., 200\}$. $t_{\max}$ and $t_{\min}$ are the maximum and minimum values of computation time; Γ_i is the normalized value of t_i. Ψ_i is the normalized value of E_i. $E_{\max}$ and $E_{\min}$ are the maximum and minimum values of RMSE. The final evaluation value is calculated by summing the normalized values of the computation time and the RMSE, and then the optimal number k_{m} of collocation points is chosen by Eqs. (20) and (21):

$$e(k_i) = \Psi_i + \Gamma_i, \quad (20)$$

$$k_{\text{m}} = \arg \min e(k_i). \quad (21)$$

3.4 Target Cruising Time at Signalized Intersection in Pre-planning and Re-planning Program

Due to the heavy load and longitudinal size of ART, the frequent start and stop when passing the signalized intersections will not only increases the travel time, but also increases the energy consumption, which greatly affects the punctuality and economy of ART. Therefore, when passing the signalized intersections, ART should avoid stopping and waiting for red lights. In order to facilitate the solution of the problem, the assumptions are made: 1) The communication delay during the information interaction between the road equipment and the onboard equipment is ignored; 2) The ART can pass the signalized intersections without being affected by other traffic participants.

Based on the assumptions above, the intersections can be regarded as destinations and the whole route is divided into several segments by the intersections. As long as the target cruising time of each segment is in the green light window, ART can pass the intersection without stopping. In order to reduce the fluctuation of velocity, the average velocity of each segment is planned to be close to the average velocity of the whole route. Meanwhile, the target cruising time should stay away from the red-light window. As a result, the target cruising time is derived from the expected cruising time and red-light window. To find the appropriate target cruising time in each segment, a potential field-based model is designed to describe the effects of expected cruising time and red light window, and the time with the lowest potential is selected as the target cruising time.

The expected cruising time during Segment i is calculated by the length of the segment and the expected average velocity of the whole route:

$$t_{\text{seg},i} = \frac{\sum_{k=1}^{i} l_{\text{seg},k}}{v_{\text{avg}}} = \frac{t_{\text{total}}}{S_{\text{f}}} \sum_{k=1}^{i} l_{\text{seg},k}, \quad (22)$$

where $l_{\text{seg},k}$ is the length of segment k; v_{avg} and t_{total} are the expected average velocity and required arrival time of the whole route between two adjacent stations, respectively. $t_{\text{seg},i}$ is the expected cruising time during segment i. The target cruising time $t_{\text{target},i}$ needs to approach the expected cruising time and stay away from the red light window. As shown in Figure 4, by comparing the summation of expected cruising time potential and red light potential, the time with the lowest potential is selected

Wang *et al. Chinese Journal of Mechanical Engineering*   (2023) 36:82

Page 8 of 13
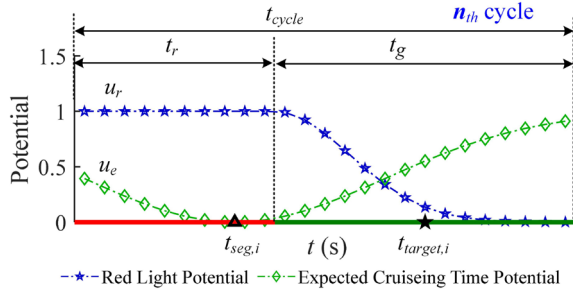
Figure 4 Selection of target cruising time at signalized inter- section in Segment *i*

as the target cruising time $t_{\text{target},i}$. When $t_{\text{seg},i}$ is in the n_{th} cycle of the traffic light, the potential field function is defined by a Gauss-type function, and the potential filed based model is given as:

$$t_{\text{target},i} = \begin{cases} t_{\text{seg},i}, & t_{\text{seg},i} \in [nt_{\text{cycle}} - t_{\text{g}}, nt_{\text{cycle}}], \\ \arg\min U(t), t_{\text{seg},i} \notin [nt_{\text{cycle}} - t_{\text{g}}, nt_{\text{cycle}}], \end{cases}$$

$$\begin{cases} U(t) = u_{\text{e}}(t) + u_{\text{r}}(t), \\ u_{\text{e}}(t) = 1 - \exp((t - t_{\text{seg},i})^2 / 2\sigma_{\text{e}}^2), \\ u_{\text{r}}(t) = \exp((t - nt_{\text{cycle}} + t_{\text{g}})^2 / 2\sigma_{\text{r}}^2 / (1 + t_{0,i}/t_{\text{seg},i})^2), \\ t \in [nt_{\text{cycle}} - t_{\text{g}}, nt_{\text{cycle}}], \end{cases}$$

(23)

where U is the potential of time. t_{r} and t_{g} are the time of red light and green light, respectively. u_{e} and u_{r} are the potentials generated by expected cruising time and red light window, respectively. σ_{e} and σ_{r} are the convergence coefficients of the potential u_e and u_r, respectively. u_{r} is related to the starting time $t_{0,i}$, which aims to avoid the too short target cruising time in re-planning program. The time interval is set to be the next cycle if $t_{\text{target},i}$ equals to nt_{cycle}.

4 Simulation Results and Analysis
Simulations are carried out to verify the effect of the proposed velocity planning method in the co-simulation environment including PreScan, TruckSim, and MATLAB/ Simulink. The driving environmental scenes of the vehicle are established in PreScan, in which the virtual sensors (such as camera, radar, GPS, etc.) mounted on the vehicle send signals to Simulink in real-time. The perception information is processed in MATLAB/Simulink through the algorithms to obtain the environmental input for controller design [40]. The control output for the actuator is calculated by the control algorithm and sent to the vehicle dynamics system in TruckSim. The real-time motion states of the dynamics system are sent to PreScan for updating the virtual scene.

The parameters of ART used in simulations are demonstrated in Table 1. In this section, the proposed ART velocity trajectory optimization algorithm is verified by simulation in the scenario with traffic lights, varying sloping and invasion of the pedestrian.

### 4.1 Selection of the Collocation Points Number
According to the road data of the operating ART, the average station spacing is no more than 2 km. For a 15 km route collected from real traffic scenarios, which is shown in Figure 5, three representative road conditions of this route are analyzed. Road 1 is simplified from the mostly flat roads. Road 2 represents the less fluctuating roads, and Road 3 represents the most fluctuating roads. The results for collocation points derived from the three representative road conditions can be applied to the whole route.

The number of collocation points is set to be distributed in $K = \{20, 30, 40, ..., 200\}$. The influences of collocation points on the real-time performance and planning results of the PS method are shown in Figure 6.

It can be seen in Figure 6(a)–(c) that when the number of the collocation points increases, the similarity of the planned velocity curves with the two methods is improved, and the computation time of the program increases. Figure 6(d) shows that the appropriate number of collocation points for a distance of 2000 m is between 60 and 100. To be concluded, the number of collocation points is chosen by the ratio of 80 points for a distance of 2000 m. This conclusion is applied to the following simulations in Section 4.
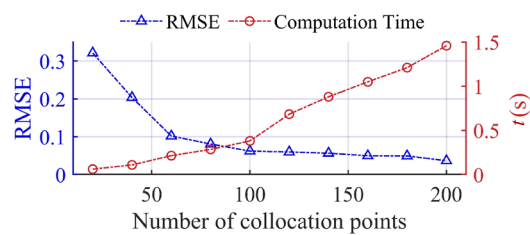
Table 1 The parameters of ART

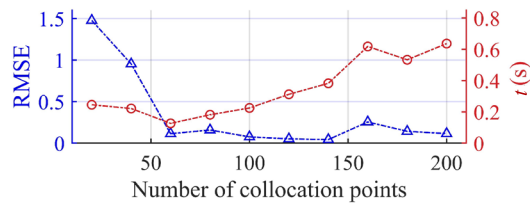| Parameter	Value
Total Mass M (kg)	40000
Tire Radius R_{t} (m)	0.54
Frontal Area A_{f} (m^2) of the First Carriage	7.98
Air Resistance Coefficient C_{d}	0.28
Rolling Resistance Coefficient f_{r}	0.015
Air Density ρ (kg/m^3)	1.202
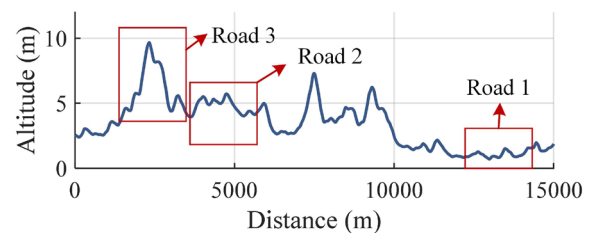
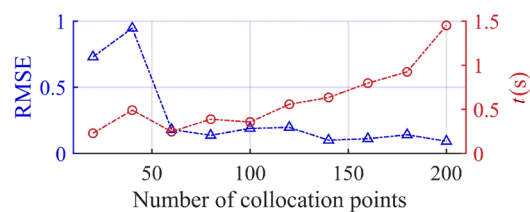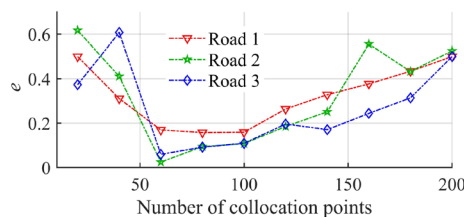**Figure 5** Road conditions with different slopes

(a) Real-time performance and planning results of Road 1

(b) Real-time performance and planning results of Road 2

(c) Real-time performance and planning results of Road 3

(d) Sum of normalized value of two evaluation indexes under different number of collocation points

Figure 6 Influence of collocation points

In order to verify the economy and punctuality of the proposed method, the velocity trajectories planned by the PDP method, the PS method, and the regular punctuality velocity (RPV) planning are compared. The target velocity of RPV is calculated by the dichotomy in the velocity range $[v_{min}, v_{max}]$. The target cruising time t_{target} is set as 290 s. The initial velocity and the terminal velocity of these three trajectories are 15 km/h. The target cruising time error t_{err} in the dichotomy program is set as 0.5 s. The parameters of travel time, energy consumption and planning time, are compared in Table 2. Figure 7 shows the velocity planning results in Road 3.

It can be seen from Figure 7 that the velocity curves obtained by the PS method and the PDP algorithm

**Table 2** Comparison of parameters of the velocity trajectories planned by different methods in Road 3

Strategy	RPV	PDP	PS
Average velocity (km/h)	24.8	24.8	24.8
Arrival Time(s)	290.4	290.3	290.0
ΔQ(kWh)	5.78	5.11	5.13
Energy saving rate (%)	Benchmark	11.56	11.39
Computation Time (s)	-	37.6	0.23

have similar trends. The PDP-based strategy can meet punctuality when α equals −3477. The velocity trajectory planned by the PS can also meet the requirements of the punctual and safe arrival of ART. Compared with the RPV, the energy consumption of the ART with the PDP method and the PS method reduces by 11.56% and 11.39%, respectively. The PS method can provide an almost equivalent energy-saving effect for the ART compared with the PDP method. From the perspective of algorithmic computation time, the PDP algorithm takes 37.6 s for the whole process. The PS method takes only 0.23 s, saving quite a lot of computation time compared with the PDP algorithm, which greatly improves planning efficiency. It is obvious that the real-time performance of the PS method is better than the PDP.

4.2 Co-simulation in Complex Traffic Scenario with Multi Traffic Lights and Random Obstacles

Generally speaking, the number of signalized intersections is less than 2 between adjacent stations. Road 3 in Section 3 is chosen to establish the scenario in the simulation. As shown in Figure 8, two traffic lights are located at 800 m and 1600 m, respectively, and the whole route is divided into 3 segments, denoted by Segment 1 to Segment 3. The timetable of the traffic light within a cycle is shown in Table 3. The altitude information and traffic light signals can be collected in advance.
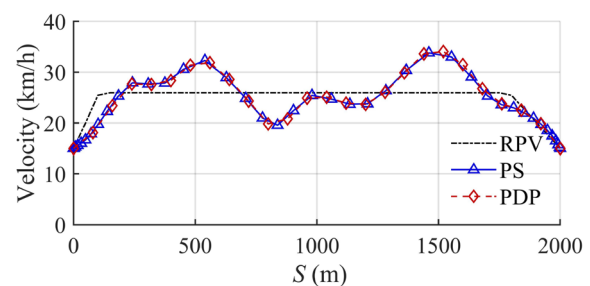
Figure 7 Velocity trajectories planned by different methods in Road 3
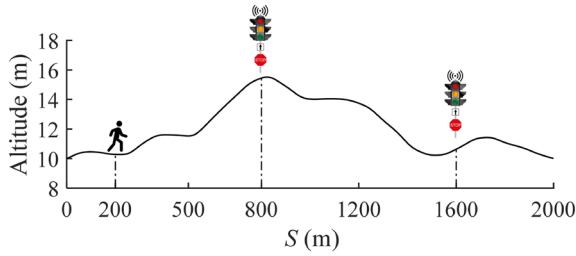
Figure 8 Typical traffic scenario in co-simulation experiment

Table 3 The time table of the traffic light in a cycle

Light Color	Time Window(s)
Red	[0, 20]
Green	[20, 50]

The velocity range is set within [5, 40] km/h. Considering the comfort of passengers and punctuality of ART, the terminal velocity interval, maximum jerk, and required arrival time are set as $v_{ter} = [15, 20]$ km/h, $j_{max} = 0.5$ m/s³, and $t_{total} = 290 \pm 5$ s, respectively.

The virtual rail of ART is constructed on the existing transport network, and the rail might be invaded by pedestrians or other low-speed vehicles, which are considered obstacles [41]. These obstacles can make ART deviate from the pre-planned velocity trajectory based on PDP. To ensure the punctuality and economy of ART, the remaining routes are re-planned with the PS method. To simulate an emergency caused by the obstacles, a pedestrian is assumed to appear at 200 m.

During Segment 1 of the route, $t_{seg,1}$ is 116 s, which is out of the green light window. In the pre-planning program, ART starts the cruise at $t_{0,1} = 0$. ART can detect the pedestrian and take the braking strategy immediately when encountering the pedestrian at a distance of 200 m. Then the remaining route is re-planned based on the PS method after the pedestrian leaves the virtual rail at 48.8 s. In the re-planning program, ART starts the cruise at $t_{0,1} = 48.8$ s. By calculating the total potential with Eq. (23), the target cruising time of Segment 1 in the pre-planning program and re-planning program can be obtained as 135 s when $t_{0,1} = 0$, and 140 s when $t_{0,1} = 48.8$ s, respectively. The target cruising time of Segment 2 can be obtained as $t_{target,2} = t_{seg,2} = 232$ s, because $t_{seg,2}$ is located in the green light window. The target cruising time of Segment 3 $t_{target,3} = 290$ s.

The proposed algorithm of velocity planning is verified in the co-simulation environment including PreScan, TruckSim, and Matlab/Simulink. In this Section, the simulation takes the traffic lights into consideration. To make the comparison more convincing, the variate, i.e. arrival time of different strategies should be the same. The commonly used speed planning method, i.e. green light optimal speed advisory (GLOSA), can ensure that ART drives into the intersection on a green signal [42, 43]. However, punctuality cannot be guaranteed if GLOSA only is adopted. A punctuality GLOSA (PGLOSA) is designed as a comparison, where the target velocity is calculated in two steps. Step 1: the target velocity range [v_{target_min}, v_{target_max}] is obtained by GLOSA in Eq. (24). Step 2: the target velocity is calculated by the dichotomy in velocity range [v_{target_min}, v_{target_max}] to meet the punctuality requirement.

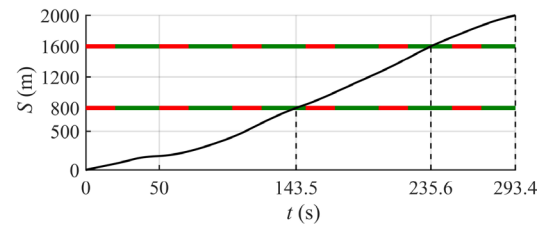$$v_{target\_max} = \min\{\frac{L}{nt_{cycle} - t_g}, v_{max}\}, v_{target\_min} = \frac{L}{nt_{cycle}},$$
$$\text{s.t.} \frac{L}{nt_{cycle}} < v_{max} < \frac{L}{(n-1)t_{cycle}},$$
(24)

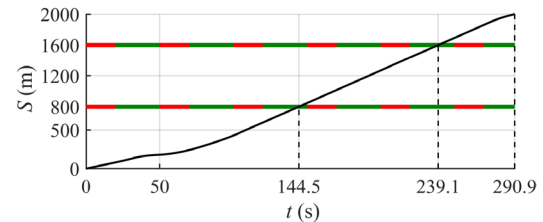where L is the distance to the traffic light. The simulation results and comparisons are as follows.

Figure 9(a) shows that the ART reaches the first signalized intersection at 153.8 s in the red light window if
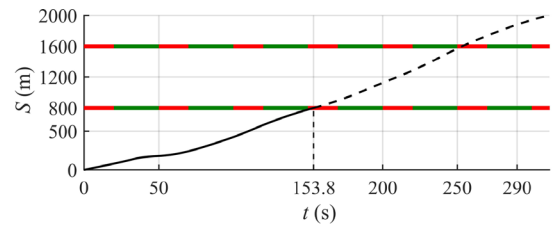
(a) Spatio-temporal trajectory without re-planning

(b) Spatio-temporal trajectory with re-planning based on PGLOSA

(c) Spatio-temporal trajectory with re-planning based on PS method

Figure 9 Comparisons of spatio-temporal trajectory

ART continues to track the pre-planning velocity without re-planning after the pedestrian leaves. On the other hand, in Figure 9(b)–(c), ART passes the first signalized intersection at 143.5 s and 144.5 s with the re-planning velocity trajectory based on PGLOSA and PS method, respectively, which are both in the green light windows.
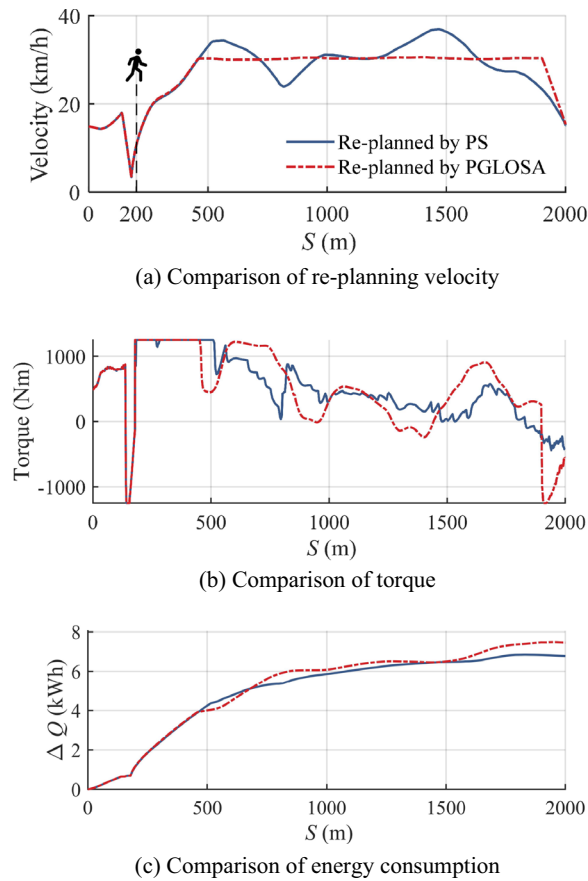
As shown in Figure 10(a), the re-planning velocity based on the PS method varies with the change of slope. The comparison of the output torque of the two re-planning strategies is shown in Figure 10(b). It can be seen from the figure that the motor output torque of the PS method-based re-planning strategy is smoother than that of the PGLOSA-based re-planning strategy. Furthermore, Figure 10(c) demonstrates that the energy consumption of the PS method-based re-planning strategy is lower than the PGLOSA-based re-planning strategy, which is 6.77 kWh for the PS method and 7.46 kWh for the PGLOSA method.

Simulation results demonstrate that, after re-planning the velocity based on the PS method, the ART arrives at the next station on time because the ART does not stop and restart while pas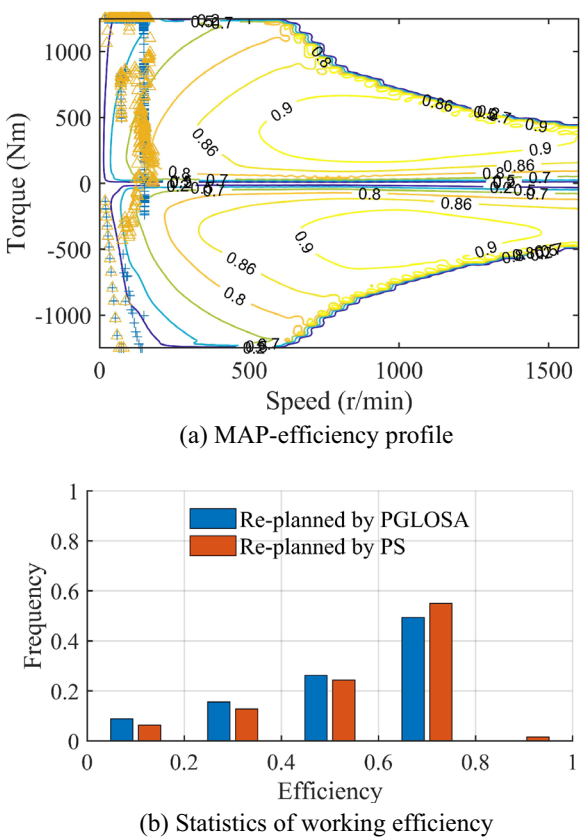sing through the intersection. As shown in Table 4, the average velocities of the ART with two re-planning strategies are 25.0 km/h and 24.5 km/h, and the corresponding arrival times are 290.9 s and 293.4 s, respectively, both meeting the requirements of punctuality. Moreover, the energy consumption of the PS-based velocity re-planning strategy has reduced by 9.19% compared with the PGLOSA-based strategy. To better understand how energy saving is achieved, the MAP-efficiency profile is given in Figure 11(a), where the yellow triangle symbols and blue cross symbols represent the working points when ART follows the target velocity re-planned by PS method and PGLOSA, respectively. The frequencies of motor efficiency in different ranges during the

Table 4 Comparison of the co-simulation results

Cruising Strategy	Re-planned by PGLOSA	Re-planned by PS
Average velocity(km/h)	25.0	24.5
Arrival time(s)	290.9	293.4
ΔQ (kWh)	7.46	6.77
Energy saving rate (%)	Benchmark	9.19

(a) Comparison of re-planning velocity

(b) Comparison of torque

(c) Comparison of energy consumption

Figure 10 Comparison of two re-planning strategy

(a) MAP-efficiency profile

(b) Statistics of working efficiency

Figure 11 Distribution of motor working efficiency

simulation are counted in Figure 11(b). The statistical histogram in Figure 11(b) suggests that the re-planning speed based on the PS method makes the motor work in the high-efficiency region as much as possible, which leads to better energy efficiency.

In conclusion, ART can consume less energy and reach the next station on time by combining the PDP and PS-based velocity planning strategy.

5 Conclusions

In this paper, the PDP algorithm and PS method are combined to pre-plan and re-plan the velocity of ART considering its economy and punctuality. The main conclusions are summarized as follows.

(1) Compared with the velocity planning method based on PGLOSA, results of PDP-based planning show lower energy consumption but a higher computation burden. By applying PDP to determine the optimal number of the collocation points for the real-time PS method and optimize the energy-saving effect and computation efficiency, the enhanced PS method reaches a similar planning result compared with PDP but shows far better real-time performance.

(2) The effectiveness of the proposed strategy for planning velocity trajectory combined with these two algorithms is verified in a typical traffic scenario including sloping roads, SPaT and invasion of the pedestrian. The result shows that the economic efficiency of ART is improved with a 9.19% reduction in energy consumption compared with PGLOSA and the punctuality is also adequate.

In summary, the proposed strategy has good application prospects for public transport under typical traffic scenarios. For future work, the proposed velocity pre-planning and re-planning strategies will be verified by real vehicle experiments on ART.

Authors' Information
Jinxiang Wang, born in 1979, is currently an Associate Professor with *School of Mechanical Engineering, Southeast University, China*. He received the B.S. degree in mechanical engineering and automation and the PhD degree in vehicle engineering from *Southeast University, China*, in 2002 and 2010, respectively. From 2014 to 2015, he was a Visiting Research Scholar with *Department of Mechanical and Aerospace Engineering, The Ohio State University, Columbus, OH,*
USA. His research interests include vehicle dynamics and control, assisted-driving system, and control on autonomous vehicles.

Dongming Han, born in 1998, is currently working toward M.S. degree at *School of Mechanical Engineering, Southeast University, China*. He received his B.S. degree at *School of Mechanical Engineering, Southeast University*, *China*, in 2020.

Yongjun Yan, born in 1995, is currently working toward the PhD degree in vehicle engineering from *Southeast University, China*. He received his B.S. degree in vehicle engineering from *Nanjing Agricultural University, China*, in 2017, and his M.S. degree in vehicle engineering from *Southeast University, China*, in 2020. His research interests include vehicle dynamics and control, automotive active safety control, intelligent vehicle decision-making and control, personalized driving.

Neng Liu, born in 1998, is currently working toward M.S. degree at *School of Mechanical Engineering, Southeast University, China*. He received his B.S. degree at *School of Mechanical Engineering, Southeast University, China,* in 2021.

Ning Sun, born in 1979, is currently a lecturer at *College of Automobile and Traffic Engineering, Nanjing Forestry University, China*. She received the PhD degree in vehicle engineering from *Southeast University, China,* in 2011.

Guodong Yin, born in 1976, received the Ph.D. degree in vehicle engineering from *Southeast University, China*, in 2007. From 2011 to 2012, he was a Visiting Research Scholar with *Department of Mechanical and Aerospace Engineering, Ohio State University, Columbus, OH, USA*. He is currently a Professor with *School of Mechanical Engineering, Southeast University, China*. His current research interests include vehicle dynamics and control, connected vehicles, and multiagent control.

Declarations

References
[1] M Saberi, H Hamedmoghadam, M Ashfaq, et al. A simple contagion process describes spreading of traffic jams in urban networks. *Nature Communications*, 2020, 11: 1616.
[2] Z Gao, L Yang. Energy-saving operation approaches for urban rail transit systems. *Frontiers of Engineering Management*, 2019, 6(2): 139-151.
[3] W Li, Q Peng, C Wen, et al. Integrated optimization on energy saving and quality of service of urban rail transit system. *Journal of Advanced Transportation*, 2020: 1-22.
[4] L Xiao, S Y Guo, X W Yuan, et al. Analysis of vision based automatic steering control for an articulated all wheel steered vehicle. *2016 IEEE Vehicle Power and Propulsion Conference (VPPC)*, 2016: 1-5.
[5] X Yuan, R Huang, X Zhang, et al. Development and validation of an automatic steering control system for rubber-tire transit revenue service. *2019 IEEE Vehicle Power and Propulsion Conference (VPPC)*, 2019: 1-6.
[6] A Sorniotti, P Barber, S De Pinto. Path tracking for automated driving: a tutorial on control system formulations and ongoing research. *Automated Driving*, 2016: 71-140.
[7] X Yang, X Li, B Ning, et al. A survey on energy-efficient train operation for urban rail transit. *IEEE Transactions on Intelligent Transportation Systems*, 2016, 17(1): 2-13.
[8] S Su, T Tang, X Li. Driving strategy optimization for trains in subway systems. *Proceedings of the Institution of Mechanical Engineers, Part F: Journal of Rail and Rapid Transit*, 2016, 232(2): 369-383.
[9] K Bao, S Lu, F Xue, et al. Optimization for train speed trajectory based on Pontryagin's maximum principle. *2017 IEEE 20th International Conference on Intelligent Transportation Systems (ITSC)*, 2017: 1-6.

[10] S Uebel, N Murgovski, C Tempelhahn et al. Optimal energy management and velocity control of hybrid electric vehicles. *IEEE Transactions on Vehicular Technology*, 2018, 67(1): 327-337.

[11] Z Xiao, Q Wang, P Sun, et al. Real-time energy-efficient driver advisory system for high-speed trains. *IEEE Transactions on Transportation Electrification*, 2021, 7(4): 3163-3172.

[12] S Su, X Wang, Y Cao, et al. An energy-efficient train operation approach by integrating the metro timetabling and eco-driving. *IEEE Transactions on Intelligent Transportation Systems*, 2020, 21(10): 4252-4268.

[13] Y Huang, L Yang, T Tang, et al. Train speed profile optimization with on-board energy storage devices: A dynamic programming based approach. *Computers & Industrial Engineering*, 2018, 126: 149-164.

[14] J Haahr, D Pisinger, M Sabbaghian. A dynamic programming approach for optimizing train speed profiles with speed restrictions and passage points. *Transportation Research Part B: Methodological*, 2017, 99: 167-182.

[15] E Hellström, M Ivarsson, J Åslund, et al. Look-ahead control for heavy trucks to minimize trip time and fuel consumption. *Control Engineering Practice*, 2009, 17(2): 245-254.

[16] M Zhou, H Jin, F Ding. Minimizing vehicle fuel consumption on hilly roads based on dynamic programming. *Advances in Mechanical Engineering*, 2017, 9(5): 168781401769411.

[17] W Zhuang, L Qu, S Xu, et al. Integrated energy-oriented cruising control of electric vehicle on highway with varying slopes considering battery aging. *Science China Technological Sciences*, 2019, 63(1): 155-165.

[18] B Asadi, A Vahidi. Predictive cruise control: utilizing upcoming traffic signal information for improving fuel economy and reducing trip time. *IEEE Transactions on Control Systems Technology*, 2011, 19(3): 707-714.

[19] M F Ozkan, Y Ma. A predictive control design with speed previewing information for vehicle fuel efficiency improvement. *2020 American Control Conference (ACC)*, 2020: 2312-2317.

[20] S Xu, H Peng. Design and comparison of fuel-saving speed planning algorithms for automated vehicles. *IEEE Access*, 2018, 6: 9070-9080.

[21] S E Li, Q Guo, S Xu, et al. Performance enhanced predictive control for adaptive cruise control system considering road elevation information. *IEEE Transactions on Intelligent Vehicles*, 2017, 2(3): 150–160.

[22] Y Yan, J Wang, K Zhang, et al. Driver's individual risk perception-based trajectory planning: A human-like method. *IEEE Transactions on Intelligent Transportation Systems*, 2022, 23(11): 20413-20428.

[23] Y Wang, B De Schutter, T van den Boom, et al. Optimal trajectory planning for trains – A pseudospectral method and a mixed integer linear programming approach. *Transportation Research Part C: Emerging Technologies*, 2013, 29: 97-114.

[24] Z Xiao, Q Wang, P Sun, et al. Modeling and energy-optimal control for high-speed trains. *IEEE Transactions on Transportation Electrification*, 2020, 6(2): 797-807.

[25] S Xu, K Deng, S E Li, et al. Legendre pseudospectral computation of optimal speed profiles for vehicle eco-driving system. *2014 IEEE Intelligent Vehicles Symposium Proceedings*, 2014: 1103-1108.

[26] S E Li, S Xu, X Huang, et al. Eco-departure of connected vehicles with V2X communication at signalized intersections. *IEEE Transactions on Vehicular Technology*, 2015, 64(12): 5439-5449.

[27] Q Lin, S Li, X Du, et al. Minimize the fuel consumption of connected vehicles between two red-signalized intersections in urban traffic. *IEEE Transactions on Vehicular Technology*, 2018, 67(10): 9060-9072.

[28] Y Liu, K Fan, Q Ouyang. Intelligent traction control method based on model predictive fuzzy PID control and online optimization for permanent magnetic maglev trains. *IEEE Access*, 2021, 9: 29032-29046.

[29] Y Cao, Z Wang, F Liu, et al. Bio-inspired speed curve optimization and sliding mode tracking control for subway trains. *IEEE Transactions on Vehicular Technology*, 2019, 68(7): 6331-6342.

[30] L Wang, X Wang, K Liu, et al. Multi-objective hybrid optimization algorithm using a comprehensive learning strategy for automatic train operation. *Energies*, 2019, 12(10): 1882.

[31] H Tang, Q Wang, X Feng. Robust stochastic control for high-speed trains with nonlinearity, parametric uncertainty, and multiple time-varying delays. *IEEE Transactions on Intelligent Transportation Systems*, 2018, 19(4): 1027-1037.

[32] Y Chen, D Huang, T Huang, et al. Tracking control via iterative learning for high-speed trains with distributed input constraints. *IEEE Access*, 2019, 7: 84591-84601.

[33] X Yan, B Cai, B Ning, et al. Moving horizon optimization of dynamic trajectory planning for high-speed train operation. *IEEE Transactions on Intelligent Transportation Systems*, 2016, 17(5): 1258-1270.

[34] W Wang, X Zeng, T Shen, et al. Energy-efficient speed profile optimization for urban rail transit with considerations on train length. *2018 21st International Conference on Intelligent Transportation Systems (ITSC)*, 2018: 1585-1591.

[35] M Wu, J Wang, Y Yan, et al. Velocity trajectory planning of the autonomous-rail rapid tram considering terrain and traffic lights. *2020 IEEE 23rd International Conference on Intelligent Transportation Systems (ITSC)*, 2020: 1-6.

[36] J Han, A Sciarretta, L L Ojeda et al. Safe- and eco-driving control for connected and automated electric vehicles using analytical state-constrained optimal solution. *IEEE Transactions on Intelligent Vehicles*, 2018, 3(2): 163-172.

[37] A Sciarretta, G De Nunzio, L L Ojeda. Optimal ecodriving control: energy-efficient driving of road vehicles as an optimal control problem. *IEEE Control Systems Magazine*, 2015, 35(5): 71-90.

[38] G Elnagar, M A Kazemi, M Razzaghi. The pseudospectral Legendre method for discretizing optimal control problems. *IEEE Transactions on Automatic Control*, 1995, 40(10): 1793-1796.

[39] F Fahroo, I Ross. Advances in pseudospectral methods for optimal control. *AIAA Guidance, Navigation and Control Conference and Exhibit*, 2008.

[40] J Wang, Y Yan, K Zhang, et al, Path planning on large curvature roads using driver-vehicle-road system based on the kinematic vehicle model, *IEEE Transactions on Vehicular Technology*, 2021, 71(1): 311-325.

[41] Y Yan, J Wang, Y Wang, et al. A cooperative trajectory planning system based on the passengers' individual preferences of aggressiveness, *IEEE Transactions on Vehicular Technology*, 2023, 72(1): 395-406.

[42] X Tang, Z Duan, X Hu, et al. Improving ride comfort and fuel economy of connected hybrid electric vehicles based on traffic signals and real road information. *IEEE Transactions on Vehicular Technology*, 2021, 70(4): 3101-3112.

[43] H Dong, W Zhuang, B Chen, et al. Enhanced eco-approach control of connected electric vehicles at signalized intersection with queue discharge prediction. *IEEE Transactions on Vehicular Technology*, 2021, 70(6): 5457-5469.